Model Experiment of Magnetic Field Amplification in Laser-Produced plasmas via the Richtmyer-Meshkov instability

Y. Kuramitsu,[1, a)] N. Ohnishi,[2] Y. Sakawa,[3] T. Morita,[3, b)] H. Tanji,[4] T. Ide,[4] K. Nishio,[5] C. D. Gregory,[6, c)] J. N. Waugh,[6] N. Booth,[7] R. Heathcote,[7] C. Murphy,[8] G. Gregori,[8] J. Smallcombe,[6] C. Barton,[6] A. Dizière,[9] M. Koenig,[9, 10] N. Woolsey,[6] Y. Matsumoto,[11] A Mizuta,[12] T. Sugiyama,[13] S. Matsukiyo,[14] T. Moritaka,[1] T. Sano,[3] and H. Takabe[15]

[1)] *Department of Physics, National Central University, No. 300, Jhongda Rd., Jhongli, Taoyuan, 320 Taiwan*

[2)] *Department of Aerospace Engineering, Tohoku University, 6-6-01 Aramakiazaaoba, Aoba-ku, Sendai, 980-8579 Japan*

[3)] *Institute of Laser Engineering, Osaka University, 2-6 Yamadaoka, Suita, Osaka, 565-0871 Japan*

[4)] *Graduate School of Engineering, Osaka University, 2-1, Yamadaoka, Suita, Osaka 565-0871, Japan*

[5)] *Graduate School of Science, Osaka University, 1-1 Machikaneyama-cho,Toyonaka, Osaka 560-0043, Japan*

[6)] *York Plasma Institute, Department of Physics, University of York, York, YO10 5DD, UK*

[7)] *Rutherford Appleton Laboratory, Chilton, Didcot OX11 0QX, UK*

[8)] *Department of Physics, University of Oxford, Parks Road, Oxford OX1 3PU, UK*

[9)] *LULI - CNRS, Ecole Polytechnique, CEA : Université Paris-Saclay ; UPMC Univ Paris 06 : Sorbonne Universités - F-91128 Palaiseau cedex, France*

[10)] *Institute for Academic Initiatives, Osaka University, Suita, Osaka 565-0871, Japan*

[11)] *Graduate School of Science, Chiba University, 1-33 Yayoi-cho, Inage-ku, Chiba 263-8522, Japan*

[12)] *Computational Astrophysics Laboratory, RIKEN, Wako 351-0198, Japan*

[13)] *Japan Agency for Marine-Earth Science and Technology, Yokohama,*

Kanagawa 236-0001, Japan

14)*Department of Earth System Science and Technology,*

Kyushu University, 6-1 Kasuga-Koen, Kasuga, 816-8580, Fukuoka,

Japan

15)*Helmholtz-Zentrum Dresden-Rossendorf, Bautzner Landstr. 400, 01328 Dresden,*

Germany

A model experiment of magnetic field amplification (MFA) via the Richtmyer-Meshkov instability (RMI) in supernova remnants (SNRs) was performed using a high-power laser. In order to account for very-fast acceleration of cosmic rays observed in SNRs, it is considered that the magnetic field has to be amplified by orders of magnitude from its background level. A possible mechanism for the MFA in SNRs is stretching and mixing of the magnetic field via the RMI when shock waves pass through dense molecular clouds in interstellar media. In order to model the astrophysical phenomenon in laboratories, there are three necessary factors for the RMI to be operative: a shock wave, an external magnetic field, and density inhomogeneity. By irradiating a double-foil target with several laser beams with focal spot displacement under influence of an external magnetic field, shock waves were excited and passed through the density inhomogeneity. Radiative hydrodynamic simulations show that the inhomogeneous density structure results in the RMI evolution and that the higher MFA than that without the density inhomogeneity.

---

a)Electronic mail: yasu@ncu.edu.tw

b)Present address: Department of Advanced Energy Engineering Science, Kyushu University, 6-1 Kasuga-Koen, Kasuga, 816-8580, Fukuoka, Japan

c)Present address: Rutherford Appleton Laboratory, Chilton, Didcot OX11 0QX, UK

I. INTRODUCTION

Extremely fast acceleration of cosmic rays in a supernova remnant (SNR) was observed in Chandra X-ray images[1]. In order to account for this, the magnetic field is considered to be amplified by orders of magnitude from its background level. There are a number of theories and models discussing the magnetic field amplification (MFA) in the shock environments relevant to cosmic rays[2]. One simple idea for the MFA is the turbulent mixing of plasmas via the Richtmyer-Meskhov instability (RMI). Recent magnetohydrodynamic (MHD) simulations predict the MFA by hundreds of times over the background level via the RMI when a shock propagates through density inhomogeneities[3,4]. Although it is known that there is density inhomogeneity in interstellar media and shock waves exist in SNRs, there is no way to identify the MFA via the RMI by observations. An alternative way to directly investigate this is through laboratory experiments with lasers[5–8]. Recently the magnetic field generation in inertial confinement plasma has also been reported via the Rayleigh-Taylor instability (RTI)[9–13]. We have shown the direct evidence of MFA in the presence of turbulence[14]. However, the amplification is limited to a few times since the magnetic Reynolds number (R_m) is also a few. Here we keep the R_m large to suppress the magnetic field diffusion in order to achieve much higher MFA. Essential factors to model such an astrophysical situation where the magnetic field is amplified via the RMI are: 1) a shock wave, 2) an existing magnetic field couple to a plasma, and 3) density inhomogeneity. We have generated and investigated laser-produced collisionless shocks[15–19] using double-parallel-plane targets and high-power lasers. The RMI is a hydrodynamic instability and thus the plasma is not necessary to be collisionless. However, in order to achieve the MFA via the RMI, we have to keep the magnetic Reynolds number large to suppress the magnetic field diffusion. The dynamics of laser-produced counterstreaming plasmas in the presence of an external magnetic fields have been investigated[20–23] and a test-bed for MFA in SNRs using density inhomogeneities established[24].

In this paper we present the results from an integrated experiment including the above three factors. We established a model experiment for MFA via RMI in SNR relevant plasmas; i.e. shock propagation in a magnetized plasma with density inhomogeneity. Using optical diagnostics we observed a plasma stretching as a shock wave propagated through the density inhomogeneity. We have developed a radiative magnetohydrodynamic (RMHD) code to
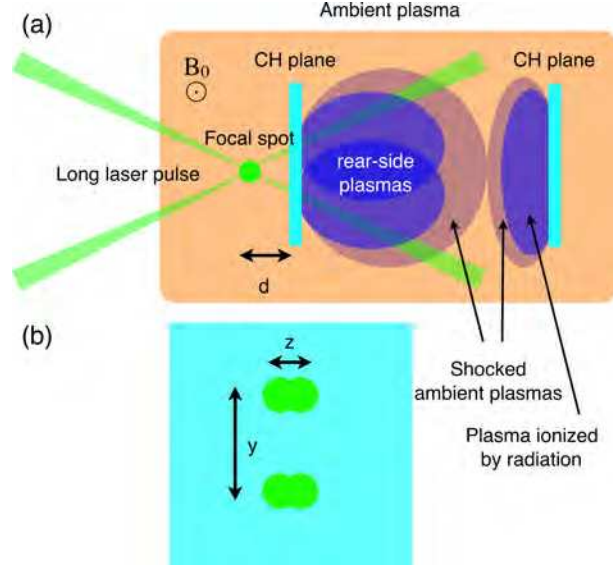
3

FIG. 1. Schematics of the target and laser configurations. (a) Side view of a double-foil target. All the beams come from the left. The beam offset is controlled by changing the distance between the focal spot and the target, d. (b) Front view of the target. The horizontal z and vertical separation y are controlled by d.

interpret the experimental results and have found we can reproduce these results if RMI occurs. As a first step toward understanding the MFA in SNRs and cosmic ray acceleration, we show a certain aspect of the RMI, resulting in the MFA. Note that these are still indirect proof of MFA; in order to understand the cosmic ray acceleration and relevant MFA, we need direct measurements of the magnetic field and the energy distribution function of the accelerated particles. These will be essential and the future issues.

II. EXPERIMENT

The experiment was performed with the Vulcan laser at the Target Area West (TAW) at the Rutherford Appleton Laboratory (RAL). We used four long pulse beams with the energy of $100 - 120$ J per beam at 2ω (527 nm). The laser pulse had a square temporal shape and duration of 1 ns and focused to spot size of 100 μm at best focus with a phase plate. The F number for each beam was 10 and the beams were arranged in rectangle pattern, where they had 12 and 50 degrees separation in the horizontal and vertical direction, respectively. At best focus, all beams clustered on the same focal spot, without moving the beams we were

4

able to alter the separation of the focal spots formed by each beam by moving the target away from best focus. Figures 1 (a) and 1 (b) schematically show the side and front view of the target. We define a coordinate system as; x axis is in the direction normal to the target rear surface, y axis is in the direction perpendicular to the x in the side view from bottom to top, and z axis is defined by the right-hand rule. We also define the plasma axis as an axis parallel to the x axis, which goes through the focal spot if the beams are best focus in Fig. 1 (a). When we move the target position away from best focus, as in Fig. 1 (a), there will be offsets of beams as depicted in Fig. 1 (b).

The target was a plastic (CH) double-foil with 5 mm separation. The first (left) foil (5 μ m) in Fig. 1 (a) is irradiated by the main beams and the second (right) foil (200 μ m) was ionized by the radiation from the first target[15–17,25]. In order to excite shock waves, a nitrogen gas jet was injected around the target environment. The gas was also ionized by the radiation from the laser-target interaction. In order to magnetize the experiment, a pulsed 3.5 T a Helmholtz coil electromagnet with inner radius of 30 mm is applied. The nitrogen gas enters before triggering magnet, followed by firing the lasers approximately 1 ms later. The magnetic field was perpendicular to the plasma axis. In the presence of the magnetic field, the ionized gas will be magnetized and be shocked by the laser produced-plasmas. As a result, shocks both from the laser irradiated left-hand foil and from the radiatively ablated right-hand foil form in the ionized nitrogen gas. These shocks are separated by a contact surface, separating target (CH) plasmas and ambient (nitrogen) plasma. Due to separation of laser focal spots on the left-hand foil a strong inhomogeneity of the left-hand shocks and contact surface results. In comparison shocks driven by radiation from right hand foil are relatively homogenous. When the shock from the right hits the inhomogeneous contact from the left, the RMI is expected to grow. The RMI stretches the contact surface due to shear flow along this surface[26], resulting in the MFA. The diagnostics were: proton radiography for the magnetic field measurement, interferometry for the electron density map and shadowgraphy for the electron distribution map. Two short (10 ps), probe beams at 1 ω were utilized for optical diagnostics.
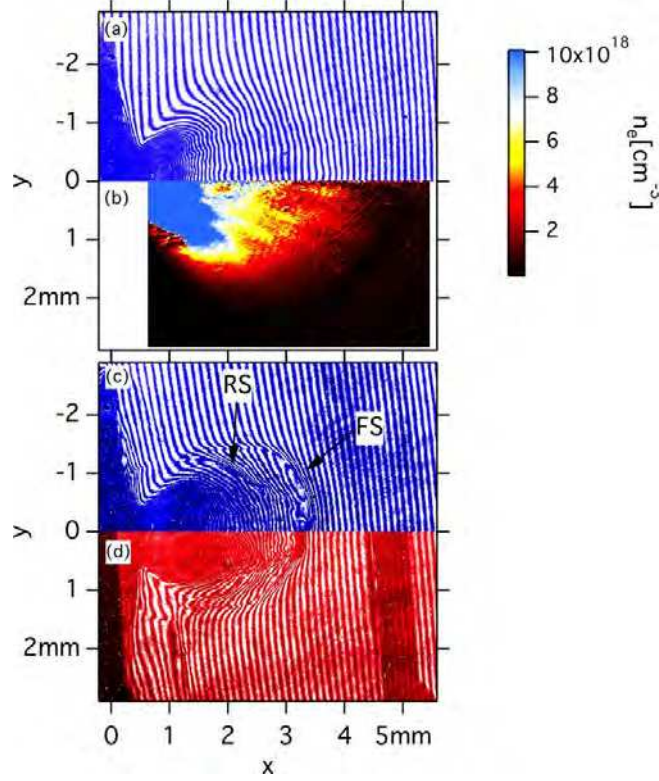
FIG. 2. I(a) Interferometry measurement of a single foil target irradiated in vacuum at best focus. (b) Electron density map inferred from (a). (c) A single foil shot taken in nitrogen plasma. The forward shocks (FS) and reverse shock (RS) are indicated. (d) A double-foil target. All measurements 10 ns after firing the long pulse beams.

III. RESULTS

Figure 2 shows reference density map and three interferograms taken 10 ns after firing four long pulse beams at best focus (i.e. with beams overlaid) and no magnetic field. In Fig. 2 (b) an Abel inverted electron density[15] inferred from the interferogram in Fig. 2 (a) is shown. The data is taken from a single foil target in vacuum. The plasma expansion is rather isotropic and the fastest plasma detectable by the interferometry is about 4.5 mm/10 ns=450 km/s with the density of $1 \times 10^{18} \text{cm}^{-3}$. With this velocity the gyro radius of proton, if in the presence of the magnetic field of 3.5 T, are 1.3 mm. Although this is not very small compared with our system size of 5 mm, the plasma is magnetized in the system.

In the presence of an ambient medium in Figs. 2 (c) a single foil target and 2 (d) a double foil target, shock waves were formed in the ambient plasma and in the target plasma,
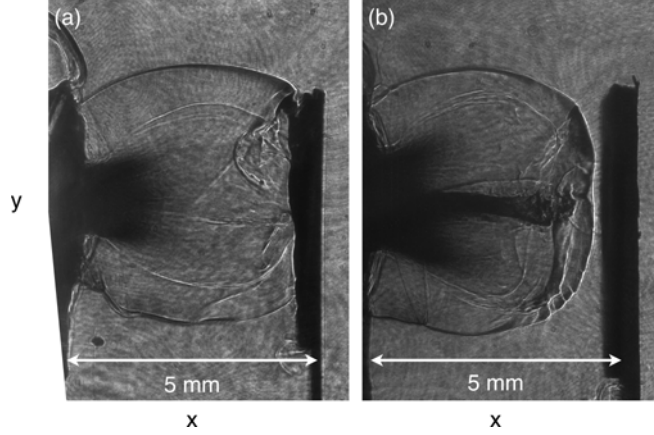
FIG. 3. Images of shadowgraphy taken at 20 ns from the laser timing. (a) Without offset ($d = 0$ mm). (b) With offset ($d = 1$ mm).

labelled as "FS" and "RS" representing forward shock and reverse shock, respectively. In Fig. 2 (d) the shadow of the right foil is seen at $x \sim 5$ mm. Since the right foil is not directly irradiated with the laser, but ionized by the radiation, the plasma velocity from the right foil is slow[17]. Consequently, the shock in the ambient plasma from the right (see schematics in Fig. 1) is expected to be weak and not discernible in the interferogram in Fig. 2 (d). However, the forward shock is slightly slower (330 km/s) than that in Fig. 2 (c) where there is no right foil (350 km/s), this indicates that the presence of the right foil affects the nitrogen plasma and propagation of the shock launched from the left foil. While the forward shock seems affected by the plasma from the right plane, it is not clear for the reverse shocks. The reverse shocks have similar velocity ~ 290 km/s in the single and double-foil experiments. The upstreams of the reverse shocks are ideally equivalent to the plasma in the vacuum in Fig. 2 (b). Thus, the density in the upstream region taken from Fig. 2 (b) is $n_{e,lu} \sim 5 \times 10^{18}$cm^{-3}. The upstream dynamic pressure $K_{ru} \equiv n_i m_i v_i^2/2$, where $n_i = n_e/Z$ is the ion density, Z is the average charge state, $m_i = A m_p$ is the ion mass, A is the mass number, m_p is the proton mass, and v_i is the ion flow velocity in the shock frame or equivalently the shock velocity in the laboratory frame, roughly equals the downstream static pressure P_{rd}. The downstream pressure of the forward shock P_{fd} has to be balanced with that of the reverse shock P_{rd} at the contact surface, and in turn the downstream static pressure is balanced by the upstream dynamic pressure of the forward shock, $P_{fd} \sim K_{fu}$. As a result, $K_{ru} \sim K_{fu}$, and thus, $n_N \sim n_{e,ru}(1/3.5)(6.5/14)(290/350)^2 = 4.6 \times 10^{17}$cm^{-3},

where we use the average values ($Z = 3.5, A = 6.5$) for CH plasma in the upstream of the reverse shock and assume $Z = 1$ for nitrogen plasma. The fringe shifts in Figs. 2 (c) and 2 (d) appear across the entire images (comparing with the reference image, not shown), indicating that the density of ambient nitrogen plasma is lower than $1 \times 10^{18} \text{cm}^{-3}$, which is consistent with the above estimate.

In the presence of the magnetic field B of 3.5 T, the gyro radius of the N^+ ion is estimated as ~ 0.25 mm assuming the N temperature of 5 eV, this temperature is based on the radiative magnetohydrodynamic (RMHD) simulations discussed below. Therefore, the ambient plasma is well magnetized and one can estimate the governing parameters in MHD limit. The Alfvén speed $c_A \equiv B/(\mu_0 n_N m_N)^{1/2} \sim 30$ km/s, where μ_0 is the permeability of the vacuum, and the Alfvén Mach number $M_A \sim 11$, which is a very strong shock. From the velocities of the forward and reverse shocks the downstream flow velocity has to be $290 < v_{fd} < 350$ km/s. Since in the laboratory frame the upstream of the forward shock is at rest, taking into account the density increase by the shock compression the mean free path of the upstream ions to the downstream ones is $0.15 < \lambda_{ii} < 0.3$ m, which is vast compared to our system size of 5 mm. Therefore, our system is collisionless. The magnetic Reynolds number is much larger than unity with the velocity of the downstream flow or of the contact surface. When the plasma is compressed or twisted, the magnetic field is amplified rather than diffuses. The plasma beta with the upstream dynamic pressure is estimated as $\beta_{fu} \equiv K_{fu}/(B^2/(2\mu_0)) \sim 135$. In the downstream region the magnetic field is amplified and then the plasma beta will be reduced.

Now we show the results with the external magnetic field. Figures 3 (a) and 3 (b) show shadowgrams taken at 20 ns from the main laser timing with and without the laser offsets, respectively. The defocusing length d were 0 and 1 mm for Fig. 3 (a) and 3 (b), respectively. Thus, the beam separations for Fig. 3 (b) were 210 μm in the z direction and 930 μm in the y direction in Fig. 1 (b). Since the beams were defocused, the spot diameter on target was ~ 200 μm. The shock propagation speed in Fig. 3 (a) is faster than that in Fig. 3 (b) (since the shock wave had already reached the right target at 20 ns in Fig. 3 (a)). The defocusing of the beams results in the lower pressure and in the slow expansion of the shock. The magnetic field direction is normal to the images. Since the plasma beta in the upstream is very large, the magnetic field is rather passive. It is clear that when beams are separated, a dense and thin structure developed on the central axis of the plasma from the left plane
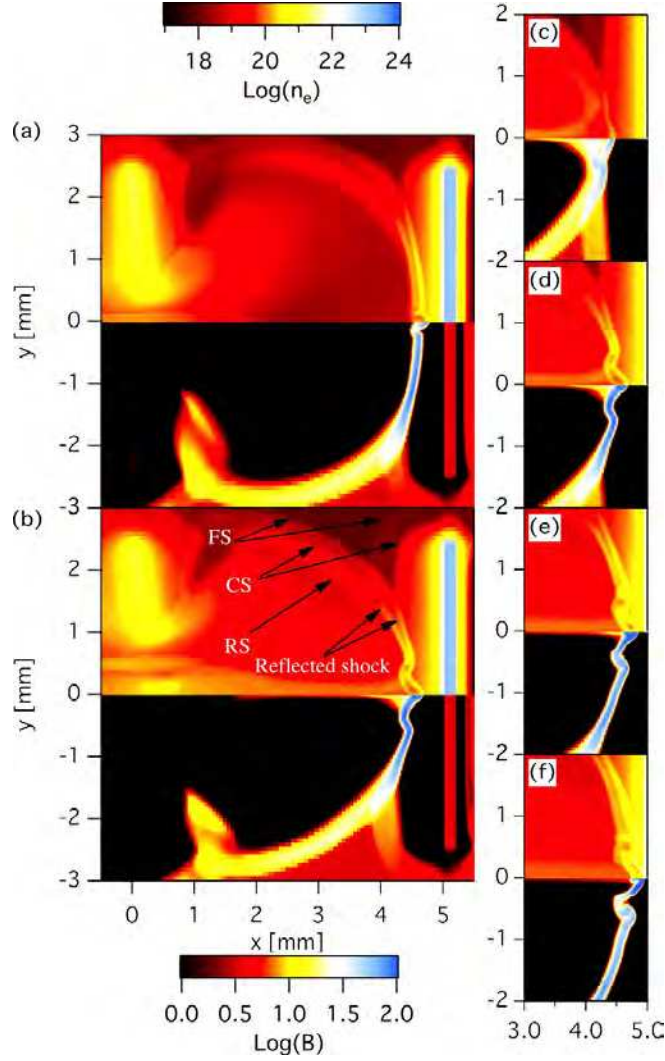
8

FIG. 4. Radiative magnetohydrodynamic simulations relevant to Fig. 3: (a) without beam offset and (b) with beam offset at 20 ns from the main laser firing. The upper and lower panels show the electron density and the z component of the magnetic field strength, respectively. The time evolution of (b) is shown in (c)–(f) at 18, 20, 22 and 24 ns, respectively. The color scales are common for all the images. The FS, RS, and CS indicate forward shock, reverse shock, and contact surface, respectively.

in Fig. 3 (b). On the other hand, when there was no beam separation, i.e., all the beam were focused on the same place, there is no such structure; the plasma expansion seems rather isotropic. In the presence of inhomogeneities, turbulent motions can be triggered in the plasma flow, in which the magnetic field can be twisted up and, in turn, amplified.

Figures 4 (a) and 4 (b) show the results from the relevant RMHD simulations without

beam offset and with beam offset, respectively, at 20 ns from the long pulses. The upper and lower panels show the density in cm^{-3} and magnetic field strength in Tesla. Figures 4 (c)– 4 (f) show the time evolution of 4 (b), at 18, 20, 22, and 24 ns, respectively. The RMHD code has been developed to include the magnetic field to the radiative hydrodynamic code in[27–29]. Note that the RMHD simulations were carried out in a two dimensional Cartesian space; in Fig. 4 the direction normal to the images is homogeneous. The two-dimensional simulations qualitatively reproduce the experimental results. These two dimensional simulations are instructive enabling detailed discussion of experimental outcomes. We leave to further work three-dimensional simulations. We see the thin structure only when we applied the beam offset, which creates the plasma inhomogeneity on the contact. In Fig. 4 (a) there is no such structure and the plasma isotropically expands. The rippled structure on the shock front near the plasma axis grows in time as the reflected shock passes through the density inhomogeneity as shown in Fig. 4 (c)–4 (f), clearly resulting from the RMI. The reflected shocks are more visible in the density (upper panels). The reflected shock might be recognized in the shadowgram in Fig. 3 (b), though there are several density structures and it is hard to determine which is the reflected shock. The magnetic field is amplified in the downstream of the reflected shock in the ambient plasma. However, the MFA is saturated at ∼ 20 ns as in Fig. 4 (b) and equivalently in 4 (d), except for the plasma axis. The strong downstream magnetic field tends to expand in Fig. 4 (d) and 4 (e), where the plasma beta is about unity (not shown), consistent with the analytical prediction in[30]. On the plasma axis the magnetic field is further amplified up to more than 300 T till the shock reach the nominal target position at 5 mm at ∼ 25 ns, just after Fig. 4 (f). On the other hand, when there is no offset, the magnetic field is amplified by shocks up to 96 T at ∼ 20 ns as in Fig. 4 (a), corresponding to the time of shock-shock interaction. There is no further MFA after this.

IV. SUMMARY AND DISCUSSIONS

A model experiment of MFA via the Richtmyer-Meskhov Instability in SNRs has been performed with Vulcan laser at the TAW/RAL. A dense and thin, filamentary structure was uniquely observed when the density inhomogeneity was introduced by the beam offsets. When there was no offset, the plasma expansion was rather isotropic and no thin feature

was observed. In order to identify the physical mechanism we have developed a RMHD code to simulate the experimental conditions. The simulations well reproduced the experimental results, showing the MFA via the RMI. In the simulation, the growth of rippled structure or the RMI seems to saturate, i.e., one cannot see the typical mushroom structure. In order to excite the RMI, the rippled contact has to be shocked; in the simulation and also in the experiment the downstream of the forward shock is compressed again by the reflected shocks. This further amplifies the downstream magnetic field and makes the downstream plasma beta of the order of unity, which is the suppression limit of the RMI[4,30]. For further MFA we have to start with even high beta, or with a weak magnetic field. Moreover, there must be free space to grow the RMI.

The dense and thin plasma structure is slightly downward. This can be caused by the laser conditions (misalignment of the laser beams and energy difference between upper and lower beams) and/or the target conditions such as the inhomogeneity of the target surface. In order to reduce these errors we need further experiments in the future.

The experimental results show the large magnetic Reynolds number, and thus, when the plasma is stretched and twisted, the magnetic field is amplified rather than diffuses. However, these are still indirect evidence of the MFA; the magnetic field measurement is needed. Proton radiography need to be modified and developed when the external magnetic field is applied. While we improve proton radiography under the influence of the external magnetic field, we have complementary tools to measure the magnetic field such as Faraday rotation[23] and magnetic field induction probes[31]. We also have tools to measure the distribution functions of accelerated particles[32,33], and we would like to investigate the particle acceleration in a RMI driven turbulence in the future.

ACKNOWLEDGMENTS

11

Astrophysical, Heliospheric, and Laboratory Collisionless Shocks. ▯

REFERENCES

[1] Y. Uchiyama, F. A. Aharonian, T. Tanaka, T. Takahashi, and Y. Maeda, Nature **449**, 576 (2007).

[2] K. M. Schure, A. R. Bell, L. O'C Drury, and A. M. Bykov, Space Sci. Rev. **173**, 491 (2012), arXiv:1203.1637 [astro-ph.HE].

[3] T. Inoue, R. Yamazaki, and S. Inutsuka, ApJ **695**, 825 (2009), arXiv:0901.0486.

[4] T. Sano, K. Nishihara, C. Matsuoka, and T. Inoue, ApJ **758**, 126 (2012), arXiv:1209.0961 [astro-ph.HE].

[5] H. Takabe, H. Nagatomo, A. Sunahara, N. Ohnishi, A. I. Mahdy, Y. Yoda, S. Naruo, H. Azechi, H. Nishimura, and K. Mima, Plasma Physics and Controlled Fusion **41**, A75 (1999).

[6] B. A. Remington, D. Arnett, R. P. Drake, and H. Takabe, Science **284**, 1488 (1999).

[7] R. P. Drake, J. Geophys. Res. **104**, 14505 (1999).

[8] B. A. Remington, R. P. Drake, and D. D. Ryutov, Reviews of Modern Physics **78**, 755 (2006).

[9] R. Betti and J. Sanz, Physical Review Letters **97**, 205002 (2006).

[10] V. Bychkov, M. Modestov, V. Akkerman, and L.-E. Eriksson, Plasma Physics and Controlled Fusion **49**, 513 (2007).

[11] M. Modestov, V. Bychkov, R. Betti, and L.-E. Eriksson, Physics of Plasmas **15**, 042703 (2008).

[12] J. R. Rygg, F. H. Séguin, C. K. Li, J. A. Frenje, M. J.-E. Manuel, R. D. Petrasso, R. Betti, J. A. Delettrez, O. V. Gotchev, J. P. Knauer, D. D. Meyerhofer, F. J. Marshall, C. Stoeckl, and W. Theobald, Science **319**, 1223 (2008).

[13] B. Srinivasan and X.-Z. Tang, Physics of Plasmas (1994-present) **19**, 082703 (2012).

[14] J. Meinecke, H. W. Doyle, F. Miniati, A. R. Bell, R. Bingham, R. Crowston, R. P. Drake, M. Fatenejad, M. Koenig, Y. Kuramitsu, C. C. Kuranz, D. Q. Lamb, D. Lee, M. J. Mac-Donald, C. D. Murphy, H.-S. Park, A. Pelka, A. Ravasio, Y. Sakawa, A. A. Schekochihin, A. Scopatz, P. Tzeferacos, W. C. Wan, N. C. Woolsey, R. Yurchak, B. Reville, and G. Gregori, Nature Physics **10**, 520 (2014).

[15]T. Morita, Y. Sakawa, Y. Kuramitsu, S. Dono, H. Aoki, H. Tanji, T. N. Kato, Y. T. Li, Y. Zhang, X. Liu, J. Y. Zhong, H. Takabe, and J. Zhang, Physics of Plasmas **17**, 122702 (2010).

[16]Y. Kuramitsu, Y. Sakawa, T. Morita, J. N. Waugh, C. D. Gregory, S. Dono, H. Aoki, H. Tanji, M. Koenig, N. Woolsey, and H. Takabe, Phys. Rev. Lett. **106**, 175002 (2011).

[17]Y. Kuramitsu, Y. Sakawa, S. Dono, C. D. Gregory, S. A. Pikuz, B. Loupias, M. Koenig, J. N. Waugh, N. Woolsey, T. Morita, T. Moritaka, T. Sano, Y. Matsumoto, A. Mizuta, N. Ohnishi, and H. Takabe, Phys. Rev. Lett. **108**, 195004 (2012).

[18]Y. Kuramitsu, Y. Sakawa, T. Morita, T. Ide, K. Nishio, H. Tanji, H. Aoki, S. Dono, C. D. Gregory, J. N. Waugh, N. Woolsey, A. Diziere, A. Pelka, A. Ravasio, B. Loupias, M. Koenig, S. A. Pikuz, Y. T. Li, Y. Zhang, X. Liu, J. Y. Zhong, J. Zhang, G. Gregori, N. Nakanii, K. Kondo, Y. Mori, E. Miura, R. Kodama, Y. Kitagawa, K. Mima, K. A. Tanaka, H. Azechi, T. Moritaka, Y. Matsumoto, T. Sano, A. Mizuta, N. Ohnishi, M. Hoshino, and H. Takabe, Plasma Physics and Controlled Fusion **54**, 124049 (2012).

[19]N. L. Kugland, D. D. Ryutov, P.-Y. Chang, R. P. Drake, G. Fiksel, D. H. Froula, S. H. Glenzer, G. Gregori, M. Grosskopf, M. Koenig, Y. Kuramitsu, C. Kuranz, M. C. Levy, E. Liang, J. Meinecke, F. Miniati, T. Morita, A. Pelka, C. Plechaty, R. Presura, A. Ravasio, B. A. Remington, B. Reville, J. S. Ross, Y. Sakawa, A. Spitkovsky, H. Takabe, and H.-S. Park, Nature Physics **8**, 809 (2012).

[20]N. C. Woolsey, Y. A. Ali, R. G. Evans, R. A. D. Grundy, S. J. Pestehe, P. G. Carolan, N. J. Conway, R. O. Dendy, P. Helander, K. G. McClements, J. G. Kirk, P. A. Norreys, M. M. Notley, and S. J. Rose, Physics of Plasmas **8**, 2439 (2001).

[21]C. Courtois, R. A. D. Grundy, A. D. Ash, D. M. Chambers, N. C. Woolsey, R. O. Dendy, and K. G. McClements, Physics of Plasmas **11**, 3386 (2004).

[22]N. C. Woolsey, C. Courtois, and R. O. Dendy, plasma physics and controlled fusion **46**, B397 (2004).

[23]H. Yoneda, T. Namiki, A. Nishida, R. Kodama, Y. Sakawa, Y. Kuramitsu, T. Morita, K. Nishio, and T. Ide, Phys. Rev. Lett. **109**, 125004 (2012).

[24]Y. Kuramitsu, Y. Sakawa, T. Morita, S. Dono, H. Aoki, H. Tanji, C. D. Gregory, J. N. Waugh, B. Loupias, M. Koenig, N. Woolsey, T. Ide, T. Sano, and H. Takabe, Ap&SS **336**, 269 (2011).

[25]Y. Kuramitsu, Y. Sakawa, J. N. Waugh, C. D. Gregory, T. Morita, S. Dono, H. Aoki,

H. Tanji, B. Loupias, M. Koenig, N. Woolsey, and H. Takabe, ApJ **707**, L137 (2009).

[26]K. Nishihara, J. K. Wouchuk, M. C., R. Ishizaki, and Z. V. V., Phil. Trans. R. Soc. A **368**, 1769 (2010).

[27]N. Ohnishi, M. Nishikino, and A. Sasaki, Journal de Physique IV **133**, 1193 (2006).

[28]N. Ohnishi, High Energy Density Physics **8**, 341 (2012).

[29]N. Ohnishi, A. Ishii, Y. Kuramitsu, T. Morita, Y. Sakawa, and H. Takabe, High Energy Density Physics **17, Part A**, 18 (2015), special Issue: 10th International Conference on High Energy Density Laboratory Astrophysics.

[30]T. Sano, T. Inoue, and K. Nishihara, Phys. Rev. Lett. **111**, 205001 (2013).

[31]G. Gregori, A. Ravasio, C. D. Murphy, K. Schaar, A. Baird, A. R. Bell, A. Benuzzi-Mounaix, R. Bingham, C. Constantin, R. P. Drake, M. Edwards, E. T. Everson, C. D. Gregory, Y. Kuramitsu, W. Lau, J. Mithen, C. Niemann, H.-S. Park, B. A. Remington, B. Reville, A. P. L. Robinson, D. D. Ryutov, Y. Sakawa, S. Yang, N. C. Woolsey, M. Koenig, and F. Miniati, Nature **481**, 480 (2012).

[32]Y. Kuramitsu, N. Nakanii, K. Kondo, Y. Sakawa, Y. Mori, E. Miura, K. Tsuji, K. Kimura, S. Fukumochi, M. Kashihara, T. Tanimoto, H. Nakamura, T. Ishikura, K. Takeda, M. Tampo, R. Kodama, Y. Kitagawa, K. Mima, K. A. Tanaka, M. Hoshino, and H. Takabe, Physics of Plasmas **18**, 010701 (2011).

[33]Y. Kuramitsu, N. Nakanii, K. Kondo, Y. Sakawa, Y. Mori, E. Miura, K. Tsuji, K. Kimura, S. Fukumochi, M. Kashihara, T. Tanimoto, H. Nakamura, T. Ishikura, K. Takeda, M. Tampo, R. Kodama, Y. Kitagawa, K. Mima, K. A. Tanaka, M. Hoshino, and H. Takabe, Phys. Rev. E **83**, 026401 (2011).